Conclusions

The graphs in Fig. 1 are for p_b* vs $\bar{\chi}$ at Mach number 10. Curves 1, 4, and 5 present the calculations of this report for the perfect gas case, the real gas case with no slip effects, and the real case with slip effects. Curve 4, when compared with curve 1, indicates that the real gas effects are not very significant for the Mach number considered, which is also obvious and expected because T_{aw} is only around 4000°K. This analysis also is useful and presents a method of solving for the real gas effects with slip for the regime between the strong interaction zone and the strong slip zone, where the behavior of η with respect to ξ should be of the strong interaction zone itself for continuity purposes. Again the reduction of the boundary-layer growth due to slip effects is clearly brought out by the first-order solution. The results for the strong slip can be obtained in a similar manner.

To conclude, the small slip effects do not really change the character of η with respect to ξ, which changes only when the strong slip effects are present. The Aroesty[4] first-order results are in good agreement with the present results, indicating that his results are only for the weak slip case and for this reason the results of Kumar and Jain[1] for the strong slip are not in agreement with Aroesty's results. Real gas effects are not very significant in the Mach number 10 case, but are seen to be dominant for the Mach number 20 case as in Fig. 2.

References

[1] Kumar, A. and Jain, A. C., "Hypersonic Viscous Slip Flow over Insulated Wedges," *AIAA Journal*, Vol. 10, No. 8, Aug. 1972, pp. 1081–1083.

[2] Lighthill, M. J., "Dynamics of a Dissociating Gas," *Journal of Fluid Mechanics*, Vol. 2, Pt. 1, Jan. 1957, pp. 1–32.

[3] Pai, S. I., "Hypersonic Viscous Flow over an Insulated Wedge at an Angle of Attack," TN BN42, Inst. for Fluid Dynamics and Applied Mathematics, University of Maryland, Baltimore, 1954.

[4] Aroesty, J., "Slip Flow and Hypersonic Boundary Layers," *AIAA Journal*, Vol. 2, No. 1, Jan. 1964, pp. 189–190.

Transient Eigenfrequencies in Liquid-Filled Cylinders

ANDREW MARK*
U.S. Army Ballistic Research Laboratories, Aberdeen Proving Ground, Md.

Introduction

THE motion of liquids in rotating containers is of interest to geophysicists because of the terrestrial molten core theory and to aerospace scientists and ballisticians because liquid payloads in missiles and projectiles can present a variety of complicated flight anomalies. In many of the past investigations on this subject, the liquid motion has been the primary concern and the liquid-container interaction was not always considered.

The Ballistic Research Laboratories study the behavior of cannon-launched, liquid-filled projectiles where the total system is of interest. The liquid is contained in a right circular cylinder within the projectile. Upon launch from a cannon, the casing (cylinder) is brought to a large, finite spin in a short time and is then acted upon by liquid and aerodynamic forces, both tending to decrease casing spin. If the projectile casing nutational frequency is sufficiently close to a liquid eigenfrequency, the possibility of resonance and resulting yaw amplification exists. This type of instability can occur while the liquid is in rigid body rotation or when the liquid is spinning up.

It was the objective of this undertaking to obtain experimental evidence of projectile instability during this spin-up phase (transient instability) and to infer increase in liquid angular momentum by measuring projectile casing spin decay. This was accomplished by the use of solar aspect sensors and radar tracking. Projectiles serve as convenient vessels when studying liquid spin-up and instability under large, impulsive, axial spins and in no way detract from their results to be generally applicable to cylindrical containers.

The solar aspect sensors consist essentially of photovoltaic cells placed behind slits in the ogive portion of the projectile. The slits are oriented such that the spinning and yawing motion of the projectile may be extracted from a series of pulses produced by the cells as they sweep past the sun. The pulses are telemetered to ground and recorded on magnetic tape. Details of the technique in accomplishing the measurements are presented in Refs. 1–3.

Five liquid-filled projectiles were fired from a 155 mm gun with a muzzle velocity of 1032 ± 15 fps generating an initial spin rate of 625 ± 9 sec^{-1} and having a nominal 30 sec flight time. Three of the projectiles, with a cavity length to diameter ratio (c/a) of 4.39, were filled to 90% of their volume with water while the remaining two with a cavity length to diameter ratio of 4.90 were filled to 80%. The cavity dimensions and fill ratios were chosen because past experience dictated a stable flight for the 90% filled case and an unstable one for the 80% case.

Redundancy of experiment is dictated whenever gun launched telemetering is involved and only a sample of each case is presented here.

Spin-Up

The casing of a liquid-filled projectile is subjected to two axially oriented moments; one of liquid origin (internal) and the other aerodynamic (external). We may therefore write the conservation of angular momentum about the axial direction as

$$M_{\text{aero}} + M_{\text{liq}} = -I_a \dot{p} \tag{1}$$

where I_a is the axial moment of inertia of the casing and $\dot{p}$ is the rate of change of casing spin. After substituting the relationship for the aerodynamic moment

$$M_{\text{aero}} = \tfrac{1}{2} C_{l_p} \rho V S l^2 p \tag{2}$$

integrating and manipulating terms we obtain

$$\frac{L_{\text{liq}}}{L_{\text{liq (rigid)}}} = \frac{I_a}{I_{\text{liq}}}\left(\frac{p_0}{p} - 1\right) - \frac{Sl^2 \int_0^t (\rho V C_{l_p} p)\, d\tau}{2 I_{\text{liq}}\, p} \tag{3}$$

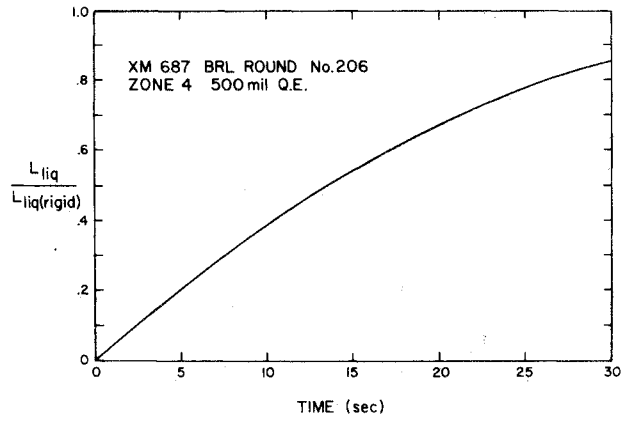

Fig. 1 Temporal increase in angular momentum of a liquid contained in a projectile.

Received February 6, 1974; revision received May 28, 1974.
Index categories: Hydrodynamics; Wave Motion and Sloshing.
* Aerospace Engineer. Member AIAA.

In this equation, L_{liq} is the instantaneous angular momentum of the liquid, I_{liq} is the axial moment of inertia for the liquid in rigid body rotation, C_{l_p} is the roll damping coefficient, ρ is the air density, V is the projectile velocity, and S and l are reference area and length, respectively. The roll damping coefficient is obtained by measuring casing spin decay of an equivalent nonliquid-filled projectile for the same flight conditions. p_0 is the spin at the muzzle. All the quantities on the right-hand side of Eq. (3) are directly measured except for I_{liq} which is calculated. We therefore have an indirect measurement of the instantaneous angular moment of a liquid in an impusively spun cylinder. Equation (3) is plotted as a function of time of flight in Fig. 1 for a representative projectile. A value of unity indicates the liquid to be at full spin. This is apparently not attained since at the end of the trajectory the ratio of angular momenta is approximately 0.85. Equivalently, this indicates that at no time throughout its flight history is the liquid at full spin and only 85% of the liquid is spinning at the end of its trajectory.

Instability

Perhaps the most descriptive solar aspect sensor measurement results pertaining to this problem are depicted in Fig. 2. The complimentary solar aspect angle is plotted as a function of time of flight. This angle is a measure of the instantaneous orientation of the longitudinal projectile axis with respect to the sun. The peak-to-peak amplitude is total projectile yaw so half that amplitude is simply the angle of attack. Data are acquired at approximately 1.5 secs and lost at 9 secs. Data loss is because the amplitude of yaw is too large and the solar aspect sensors do not see the sun any more. This occurs at an angle of attack of approximately 25°. The important portion of the data, however, is at the beginning of the flight. The precessional (slow frequency) and nutational (fast frequency) motions are clearly indicated and at data acquisition (1.5 secs from time of muzzle exit), the angle of attack is already diverging and the projectile is nutationally unstable. This implies that the projectile has already become unstable well within the liquid spin-up phase. The long time for the liquid to come to the full spin as indicated by the experimental results suggests that there is a considerable length of time during which a set of transient eigenfrequencies can act to undamp the projectile.

The upper bound on the eigenfrequencies in a partially or fully liquid-filled, spinning, circularly cylindrical cavity is given by Stewartson.[4] In his analysis, the cylinder-liquid system is spun at a fixed rate for a long enough period of time such that the liquid attains rigid body rotation. The system is then perturbed from its sleeping position. The linearized, inviscid, incompressible Navier-Stokes equations that apply result in an

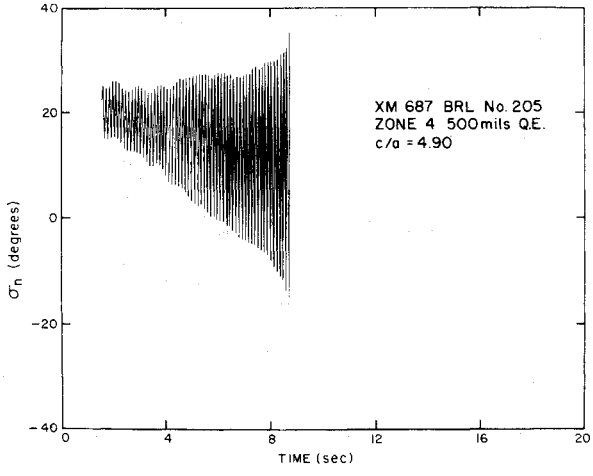

Fig. 2 Measured early onset of instability of a liquid-filled projectile.

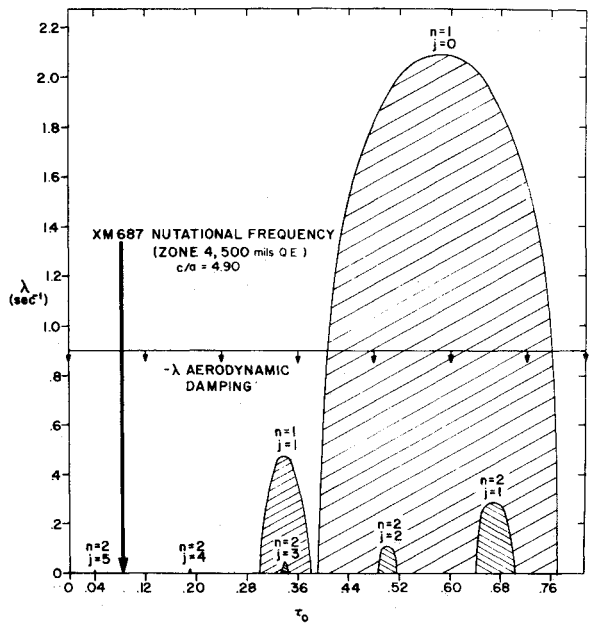

Fig. 3 Stewartson stability regions for a projectile containing liquid in a circularly cylindrical cavity.

eigenvalue problem. Although his analysis is for a spinning top, it is directly applicable to any circularly cylindrical geometry; e.g., projectiles. The governing equations for the projectile motion are augmented only in the sense that the total moment on the projectile includes both the aerodynamic moment plus the antisymmetric liquid moment. The projectile characteristic equation then takes the form

$$I_t\tau^2 - I_a\tau + (C/p^2) = D(\tau)/(\tau - \tau_0) \tag{4}$$

In this equation, I_t is the transverse moment of inertia of the casing, C is an aerodynamic coefficient, $D(\tau)$ is the liquid forcing function, τ is the yawing frequency nondimensionalized by spin and τ_0 is an eigenfrequency. When the projectile is empty, $D = 0$ and Eq. (4) yields the well-known solution for the nutational and precessional frequencies. However, when $D \neq 0$ and the mass of the liquid is small compared to that of its container, the right hand side of Eq. (4) is negligible except near $\tau = \tau_0$. Therefore, we are interested in solutions when $D(\tau) = D(\tau_0)$ and since D is always negative the criterion for instability becomes

$$|\tau_n - \tau_0| < \left\{\frac{-4D(\tau_0)}{I_a(1 - 4I_tC/I_ap)^{1/2}}\right\}^{1/2} \tag{5}$$

The rate of undamping due to the liquid is then obtained by solving the projectile yaw equation.[5] The complete stability solution consists of a series of semiellipses which are regions of instability. These are depicted in Fig. 3 for our cavity geometry. A nutational frequency falling within these regions would tend to undamp the projectile provided the aerodynamic damping were sufficiently small. This is apparently not the case for our situation as the first radial mode, $n = 1$, which is the only mode exceeding aerodynamic damping, is far removed from the projectile nutational frequency. Yet, as indicated in Fig. 2, an instability does occur and we can only conclude that the projectile nutational frequency ($\tau_n = 0.086$) encountered an instability region as the liquid increased in angular momentum from its original quiescent state. Lower bound eigenfrequencies are obtained from the well known Dirichlet problem,[6] the primary eigenfrequency mode for our geometry being $\tau_0 = 0.030$. These lower bound eigenfrequencies are below our projectile nutational frequency and monotonically increase to the Stewartson predicted upper bound as the liquid spins up. Thus they must at some point during spin-up resonate with the nutational frequency. Indeed, this is the indication in Fig. 2.

Conclusion

The behavior of liquid-filled projectiles over long flight paths is well determined by the use of solar aspect sensing and FM/FM telemetry. Transient eigenfrequencies have been experimentally demonstrated to exist for appropriate cavity geometry and fill. A slow angular momentum interchange between the liquid and casing increases the probability of projectile undamping by allowing the casing nutational frequency to hover in the vicinity of the primary eigenfrequency mode.

References

[1] Mermagen, W. H., "Miniature Telemetry Systems for Gun-Launched Instrumentation," *Proceedings of the Fourteenth International ISA Aerospace Instrumentation Symposium*, Instrument Society of America, Vol. 14, 1968.

[2] Mermagen, W. H., "Measurements of the Dynamical Behavior of Projectiles over Long Flight Paths," *Journal of Spacecraft and Rockets*, Vol. 8, No. 4, April 1971, pp. 380–385.

[3] Clay, W. H., "A Precision Yawsonde Calibration Technique," BRL Memo. Rept. 2263, AD 758158, Jan. 1973, U.S. Army Ballistic Research Labs., Aberdeen Proving Ground, Md.

[4] Stewartson, K., "On the Stability of a Spinning Top Containing Liquid," *Journal of Fluid Mechanics*, Vol. 4, Pt. 4, Sept. 1959, pp. 577–592.

[5] Murphy, C. H., "Free Flight Motion of Symmetric Missiles," BRL Rept. 1216, AD 442757, July 1963, U.S. Army Ballistic Research Labs., Aberdeen Proving Ground, Md.

[6] Lamb, H., *Hydrodynamics*, Dover, New York, 1945.

Electrical Resistivity of Gallium-Bismuth Solidified in Free Fall

LEWIS L. LACY*
NASA Marshall Space Flight Center, Huntsville, Ala.
AND
GUENTHER H. OTTO†
The University of Alabama in Huntsville, Huntsville, Ala.

Introduction

IMMISCIBLE materials in their liquid state may be defined as two or more component alloys which are mutually insoluble at a given temperature and pressure. A study of existing phase diagrams[1] reveals that there are about 500 binary liquid immiscible systems occurring between two metals or metals mixed with metallic oxides, indicating that the phenomenon of immiscibility is rather common. Despite their immiscibility, two liquid metals may be mixed to form a dispersion. In this case, one of the fluids generally breaks up into small droplets which are dispersed into the second fluid that forms the host or matrix phase. However, since the two liquid metals usually have different densities, gravity-induced segregation will occur, and the two components will finally separate by coalescence. If the dispersion is performed in a zero-g environment, density segregation does not occur, and a uniform and stable dispersion can be obtained as demonstrated recently with an experiment on Skylab.[2] Appropriately chosen material combinations can then be solidified in a low-gravity field to yield unique composite alloys, as demonstrated by experiments performed on Apollo 14,[3] Skylab,[4] and the Marshall Space Flight Center (MSFC) drop tower.[5,6]

We will report the unusual temperature dependence of the electrical resistivity found on gallium-bismuth immiscible alloys which were solidified during free fall conditions in a drop tower. The interesting superconducting properties of zero-gravity processed Ga-Bi can be found in Ref. 6.

Presented as Paper 74-208 at the AIAA 12th Aerospace Sciences Meeting, Washington, D.C., January 30–February 1, 1974; submitted February 4, 1974; revision received August 9, 1974. Portions of this work were supported by NASA Contract NAS8-27809.

Index categories: Materials, Properties of; Structural Composite Materials (Including Coatings); Liquid and Solid Thermophysical Properties.

* Senior Solid State Physicist, Space Sciences Laboratory.

† Assistant Research Professor, Department of Physics.

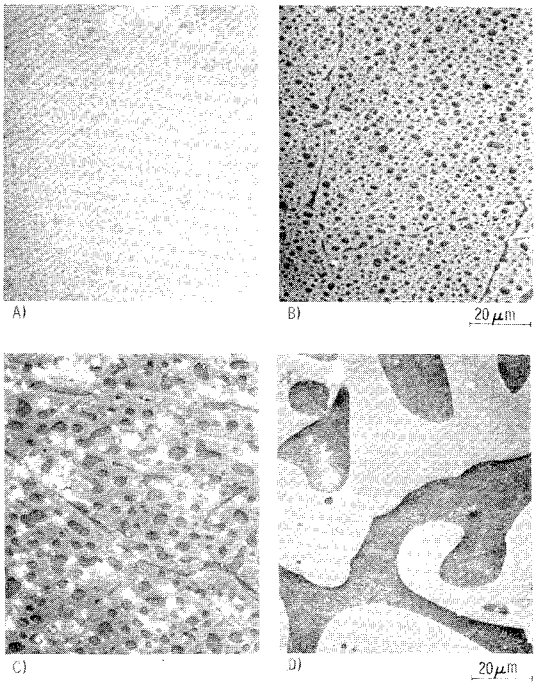

Fig. 1 Photomicrographs of the Ga-Bi immiscible alloys. Pictures A, B, and C are for free-fall solidified samples, and picture D is for a one-g sample prepared under otherwise identical conditions. The light colored areas represent the bismuth matrix whereas the dark areas are gallium particles.

Experimental Results

A simple method for obtaining a liquid dispersion of two metals without having to mechanically mix is to make use of the miscibility gap, occurring in numerous metallic constitution diagrams. Samples of Ga-Bi were processed during 4 sec of free fall in the MSFC drop tower.[7] In this time span, a single-phase metallic liquid was cooled through the liquid miscibility gap to form two liquid phases which were subsequently solidified. A ground control sample was processed under otherwise identical conditions except that the sample was not dropped. The Ga-Bi samples were processed in tantalum containers using metals with at least 99.999% purity and a concentration of 50 a/o of each element. Details of the processing procedure are given in Ref. 5.

Photomicrographs of the samples can be seen in Fig. 1, where the light-colored areas represent the Bi matrix and the darker, circular areas are the Ga. As expected, the low-g processing led to a finer and more uniform dispersion of Ga particles in a Bi matrix. The different dispersions obtained for samples A, B, and C are associated with different solidification times in zero-g. The preliminary results of these experiments indicate that the longer solidification times lead to finer dispersions.

The temperature dependence of the electrical resistivity $\rho(T)$ was measured on three dropped samples (A, B, and C) and on one ground control sample (D) by the conventional four-contact technique. A constant current of 10 mA was passed through a thin slice of the material by means of fine-spring-